Memoirs of the Faculty of Engineering,Okayama University,Vol.27, No. 1, pp.11-26, November 1992

Heat Transfer Characteristics of Two Phase Closed Thermosiphon for Geothermal Energy (1st Report: Measurement on Heat Transfer Coefficient)

Masao HIRASHIMA* and Hideo INABA**

(Received September 30 , 1992)

SYNOPSIS

To prevent freezing of road and aquaduct by extracting geothermal heat with two phase closed thermosiphon has been widely used in a cold area. Both heat transfer characteristics in the underground soil and function of the thermosiphon to extract geothermal heat have to be made clear for the purpose of the above system. This study is directed for the purpose to prevent freezing of fire hydrant and composed of the fundamental experiment and the empirical experiment. In the fundamental study, heat transfer behavior is studied experimentally in the small size filling bath representing the underground soil layer. After recording temperature distribution, heat transfer coefficient is measured, they are proceeded into the correlation between the dimensionless number of Nusselt, Rayleigh and Fourier. The fundamental study is described as the first report.

1 INTRODUCTION

The temperature of underground soil is comparably stable against the atmospheric temperature through the year. The heating and refrigerating technique by utilizing temperature difference between underground soil and

* Mitsui Metal Engineering & Service Co., Ltd.

** Department of Mechanical Engineering

atmosphere, such as snow melting of road and installationof underground cold storage is well known. Although many reports can be found out concerning comprehensive real installation[1-4], few basic studies have investigated the heat transfer mechanism in the soil containing the underground water. On the fundamental study, filled bath composed of many small glass balls and heat transfer working fluid are used to experiment heat transfer mechanism in the filled layer as a model of underground soil containing underground water. The heat is loaded with electric heater to the filled layer from the periphery of the bath and cooling tube is installed at the center of the bath as a model of heat extracting thermosiphon. The change of the temperature distribution profile in the filled layer, and heat transfer rate from the filled layer to the model thermosiphon is obtained in the basic experiment as mentioned in SYNOPSIS. Correlation between the dimensionless number obtained in the basic study is considered to be utilized for the new type of the bath composed of different kind of filling materials and working fluid in the future.

2. NOMENCLATURE

Notation

A: area (m^2)
a: thermal diffusion (m^2/h)
C: specific heat of material (kJ/kg•K)
d: diameter (m)
G: weight (kg)
g: acceleration by gravity (m/s^2)
h: heat transfer coefficient (W/m^2K)
ℓ: length (m), (mm)
Q: heat quantity (kJ)
$\dot{Q}$: heat flow rate (W)
R: electric resistance (Ω)
T, ΔT: temperature, temperature difference (^oC), (K)
v: voltage (v)
V: volume (m^3)
$\dot{V}$: volumetric flow rate (m^3/h)
β: coefficient of volumetric thermal expansion (1/K)
ρ: specific weight (kg/m^3)
λ: thermal conductivity (W/mK)
ν: kinematic viscosity (m^2/s)

Subsctipt

Dimensionless Number

e: electricity
f: fluid
i: inner
o: outer
p: particle
s: solid
w: water

Fo: Fourier Number
Gr: Grashof Number
Nu: Nusselt Number
Pr: Prandtl Number
Ra: Rayleiyh Number

3 EXPERIMENTAL APPARATUS AND PROCEDURE

3.1 Main Parts of Experimental Apparatus

Two kinds of the equipment, I and II are used as shown in Fig.1. Equipment I is filled up by 10.0mm diameter of glass balls as the filled material, and 5.0mm of glass balls are used in Equipment II. The physical property and the distribution of grading of the glass balls are shown each in Table.1 and Fig.1. Beside the glass balls as filling material, flow mechanism of the cooling water of model thermosiphon of each equipment is different. Reverse flow system of cooling water by concentric duplex pipe is employed in Equipment I and, straight flow system by single pipe is constructed in Equipment II as in Fig.2. Main parts of the both experimental apparatus are composed of electric heater, test part, and model

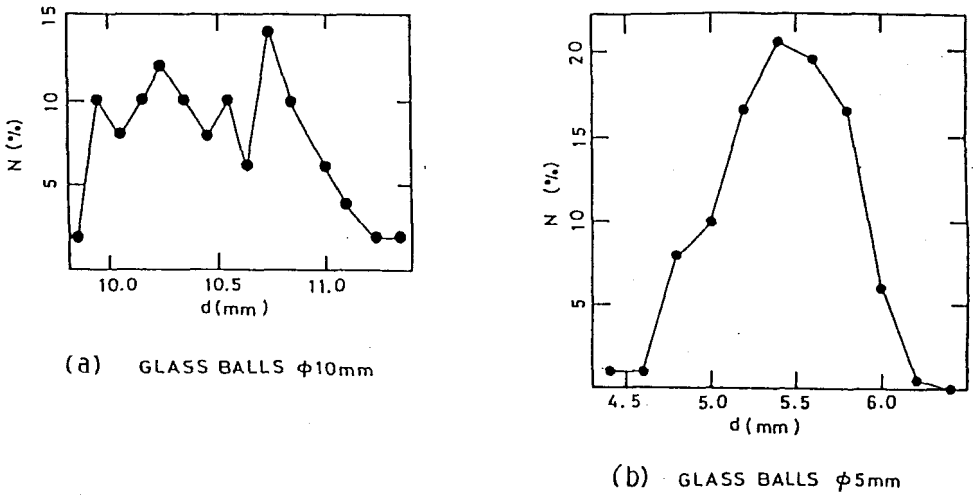

Fig.1 Diameter distribution of glass particle

Table 1 Property of filled material

Material	Nominal Dia. mm	Mean Dia. mm	Deviation mm	Coeff. of Variation %	Specific Heat kJ/(kg·K)	Specific Weight kg/m³	Thermal Conductivity W/(m·K)
Glass	10	10.412	0.3327	3.20	0.753 (20°C)	2450 (20°C)	0.74 (20°C)
	5	5.408	0.2813	5.18			

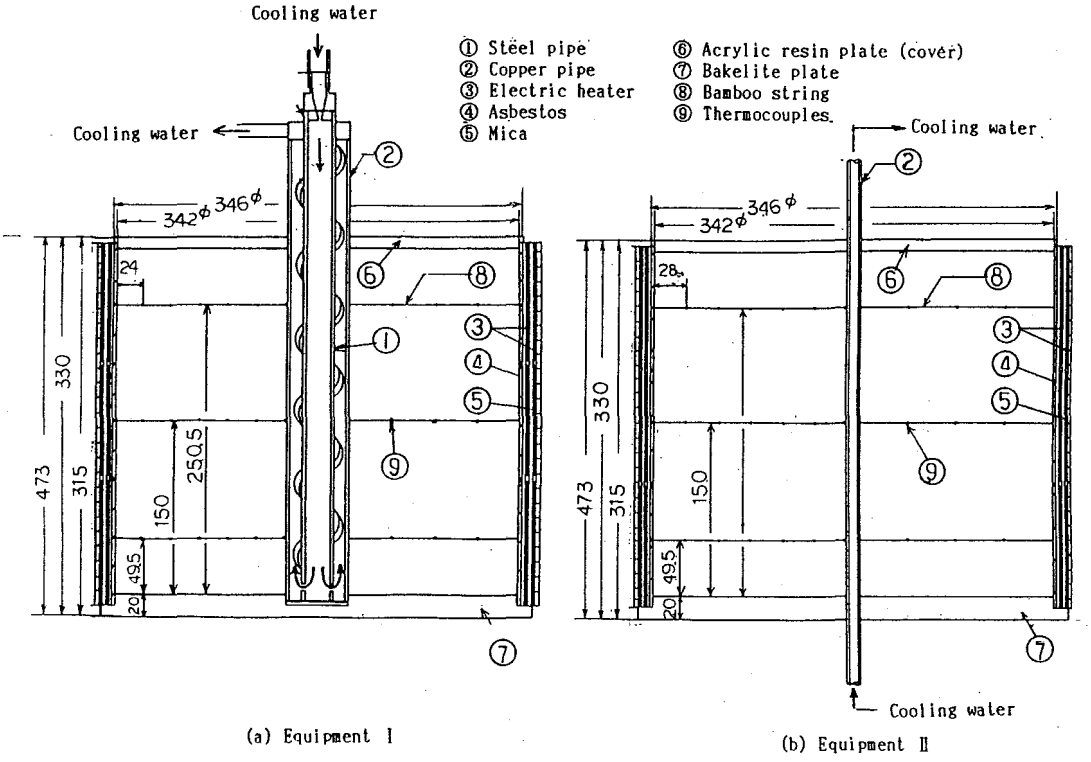

Fig.2 Cross section of the test equipment

thermosiphon as the heat sink. Main heating plate (0.2mm × 0.8mm, 7Ω/m) is divided into three groups in parallel and is located around the periphery of the test bath so that larger current and heat quantity can be attained, compared with the case of series arrangement. Outside of the main heating plate is surrounded with the auxiliary heater to eliminate heat release from the main heater to the surrounding, and the current of both heaters is adjusted by the variable transformer to maintain the constant temperature of the both heaters during the run. The

test bath is finally insulated by the asbestos sheet of 10mm thick. Upper end of the cylindrical test bath is covered by acrylic plate in operating period and bakelite plate is attached indirectly by rubber packing to the bottom of the test bath. The cooling device of the Equipment I is constructed as a duplex tube as mentioned above . The cooling water enters from the top of inner steel pipe(d_o=28.0mm, d_i=21.0mm), passes downward through the inner pipe, reverses at the bottom and goes up inside of the outer copper pipe(d_o=54.0mm, d_i=51.0mm) and then leads outside. The cooling device of the Equipment II is constructed as a single tube. The cooling water is led into copper pipe(d_o=6.0mm, d_i=4.0mm) from the bottom, passes through upward and is taken out from the top. According to the difference of the water flow mechanism in the two model thermosiphon, the axial temperature gradient of Equipment I is smaller compared with that of Equipment II.

Water, alcohol, and lubricating oil are used as the working fluid. Physical property of the working fluid is shown in Table 2.

Table 2 Property of working fluid

Material	T °C	ρ kg/m³	C kJ/(kg·K)	η kg·s/m²	ν m²/s	λ W/(m·K)	a m²/h	Pr	β 1/K
Water	20	998.2	4.182	1.03×10^{-4}	1.01×10^{-6}	0.594	5.12×10^{-4}	7.11	0.20×10^{-3}
C_2H_5OH	20	790	2.415	1.22×10^{-4}	1.51×10^{-6}	0.182	3.44×10^{-4}	15.80	1.12×10^{-3}
Oil	20	866	1.892	32.2×10^{-4}	38.5×10^{-6}	0.124	2.73×10^{-4}	481.00	0.89×10^{-3}

3.2 Heating and Cooling System of the Equipment.

As shown in Fig.3, the source of heating system is connected to the voltage stabilizer, through the twelve sliding registers and divided into each three main and auxiliary heater of Equipment I and Equipment II. The current and output of the heating plate is controlled with the above mentioned system and the heating surface is maintained in even temperature through the each run of experiment. Chilled water is delivered to each model thermosiphon which is cooled by the brine (Chilled $-5^{\circ}C \sim -20^{\circ}C$ by the refrigerator) through the heat exchanger. Ice layer is tried to form on the surface of the heat exchanger in this experiment so as to maintain the temperature of chilled water always at 0 C. According to the new trial of the above system the temperature of the cooling water maintained in constant value of $0^{\circ}C$ in spite of any load fluctuation Heating and cooling system of the experiment is schematically shown in Figs. 2 and 3.

3.3 Measuring System

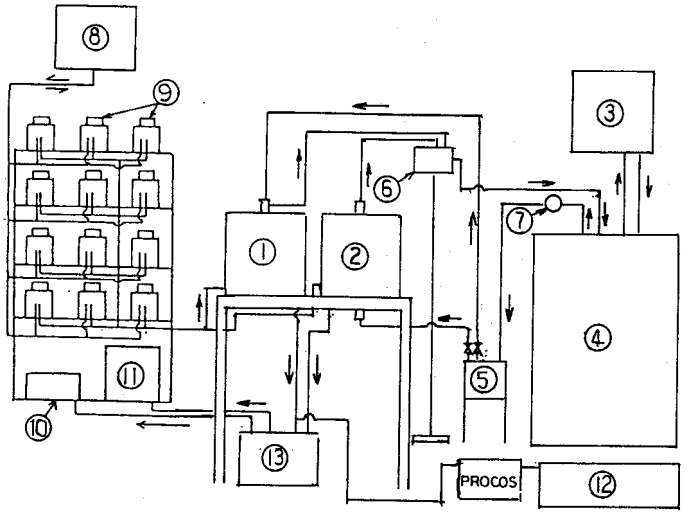

① Equipment I
② Equipment II
③ Refrigirator
④ Cooling water storage tank
⑤ Distribution tank I
⑥ Distribution tank II
⑦ Pump
⑧ Voltage stabllizer
⑨ Adjustable register
⑩ Pen recorder
⑪ Marti points recorder
⑫ Computor for temperature analying
⑬ Zero set terminal

Fig.3 Flow diagram of the test equipment

Heat output of the electric heater is calculated by equation (1)

$$Q_e = V_e^2/R_e \tag{1}$$

where V_e in equation (1) is measured by the volt meter of the voltage stabilizer and R_e is specific resistance of the main electric heater (7Ω/m). Carolific value taken out by the cooling water passing through the model thermosiphon is calculated by equation (2)

$$\dot{Q} = \frac{V_w \cdot \rho_w \cdot C_w (T_{w2} - T_{w1})}{3.6} \tag{2}$$

where V_w is measured by orifice type flow meter located at the outlet of cooling water pump, and T_{w1}, T_{w2} are the cooling water temperature of inlet and outlet of the model thermosiphon. With respect to the temperature in the filling bath, it is measured by the thirty pieces of thermocouples (C-C) which is put by ordinate method on the string made of bamboo located horizontally between the heating and cooling surface of the bath as in Fig.4.

3.4 Procedure of the Experiment.

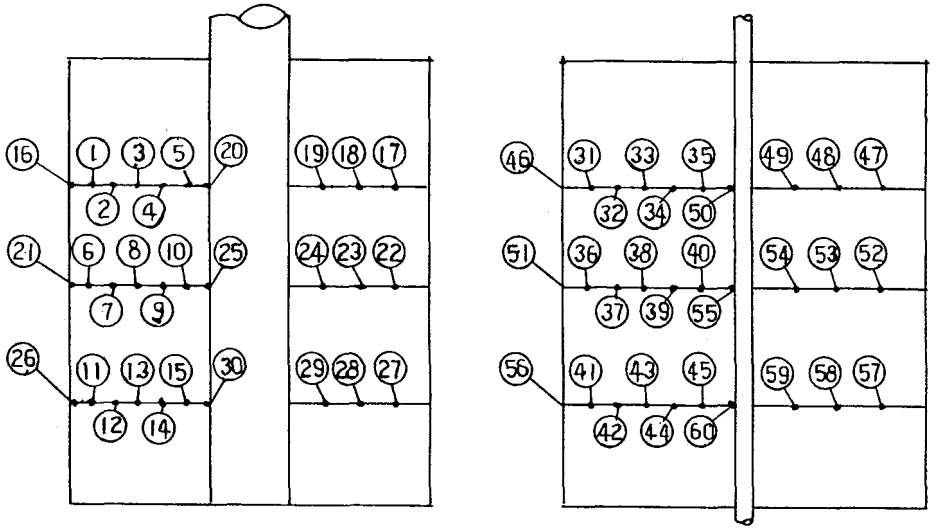

(a) Equipment I (b) Equipment II

Fig.4 Temperature measuring point

The basic condition to carry out the experiment is to maintain the temperature of heating surface and this is attained by the hand adjustable transformer as indicated in Fig.3. The purpose of this is to give the condition of constant heat flow to the thermosiphon from the surrounding underground soil as in real application. Cooling water quantity has to be maintained constant and this is achieved by adjusting the controll valve located at the outlet of the distribution tank. At first, the temperature of the heating surface is heated up to a certain value corresponding to each run number by adjusting transformer till the temperature distribution of filled layer reaches to the stable profile. Cooling water is begun introduced to the model thermosiphon when the temperature distribution of the filled layer reaches the stable state, and change of temperature of the measuring points (refer to Fig.4) is plotted along the time proceeding as in Fig.5, till the temperature distribution profile of the whole filling layer reaches the stable figure. As the experiment proceeds under the condition of unstable state, the run completes when the temperature of the heating surface does not fluctuate any more and the temperature difference between inlet and outlet of the cooling water reaches the constant value.

4. EXPERIMENTAL RESULTS AND DISCUSSION

4.1 Definition of Cavity E and Permeability S_i

It is necessary to give a definition of cavity E and permeability S_i of the filling layer prior to process the experimental data. Cavity of the filling layer E is defined in equation (3)

$$E = 1 - G_p/(\rho_p \cdot V) \tag{3}$$

for the Equipment I

$$E1 = 1 - 39/2450 \times 0.0269 = 0.408$$

for the Equipment II

$$E2 = 1 - 42/2450 \times 0.0276 = 0.379$$

as for the permeability Si, equation (4) is reffered

$$S_i = E^3 d_p^2/150(1-E)^2 \tag{4}$$

for the Equipment I

$$S_{i1} = 0.408^3 \times 0.01^2/150(1-0.408)^2 = 1.29 \times 10^{-7}$$

for the Equipment II

$$S_{i2} = 0.379^3 \times 0.005^2/150(1-0.379)^2 = 2.35 \times 10^{-8}$$

4.2 Temperature Distribution Profile in the Filling Layer and Elapsed Time

As shown in Fig.5, change of temperature of each measuring point shows common tendency along the time proceeding in all run. The temperature of the layer which contacts to the surface of the thermosiphon decreases suddenly just after the cooling water is induced to the cooling pipe, then the temperature of surrounding layer follows it slowly in order and temperature distribution of the whole layer reaches steady state by the whole system reaches thermal equilibrium after a certain time. Fig.5 shows the cases of water, alcohol for the Equipment I and water, oil, for the Equipment II. The number in Fig.5 corresponds to the measuring point in Fig.4. It is clear by Fig.5 that the temperature changes largely in the layer near the cooling surface compared with the layer located near the heating surface

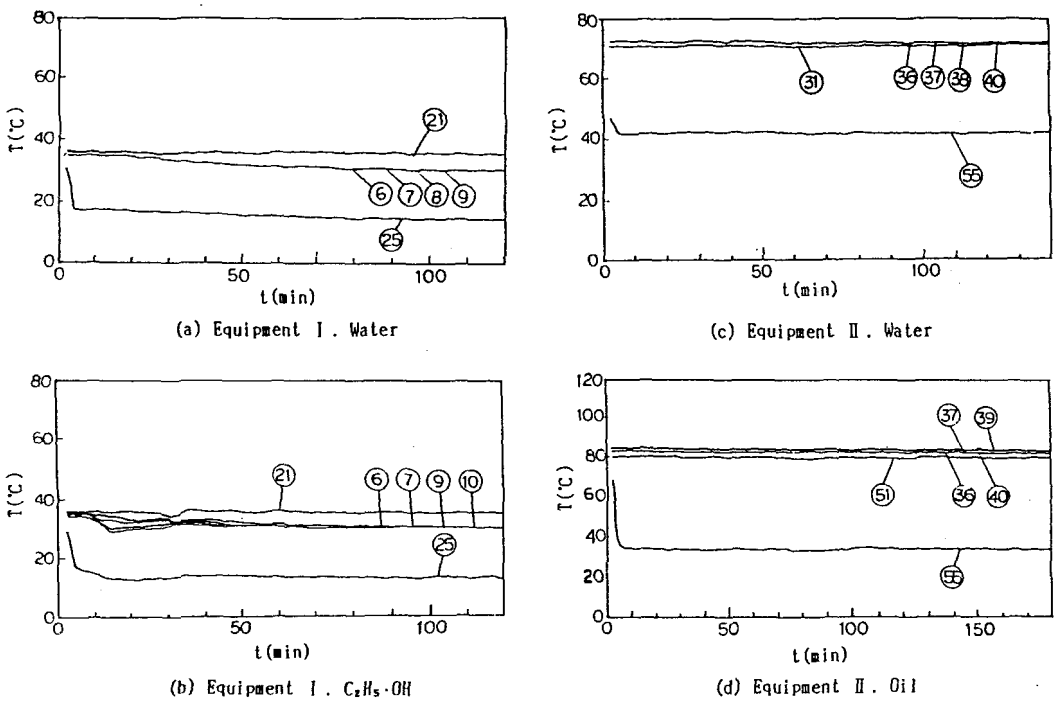

Fig.5 Temperature distribution in the bath along the time proceeding

4.3 The Relation between the Temperature Distribution and the Distance Y from the Heating Surface

Fig.6 indicates the relation between the temperature distribution and horizontal distance Y from the heating surface. The behavior of the working fluid in the filling bath is considered to depend on the viscosity of the fluid and the diameter of the glass balls. It can be observed that the temperature gradient of the water and alcohol on the axis Y (in Fig.4) is smaller compared with that of the oil, because the convection activity of water and alcohol is intensive compared with oil.

4.4 Heat Transfer Coefficient and Elapsed Time

Heat transfer coefficient between the heating surface and the cooling surface of the model thermosiphon is defined in equation (5)

$$h = Q/A_w(T_{sh} - T_{s\ell}) \tag{5}$$

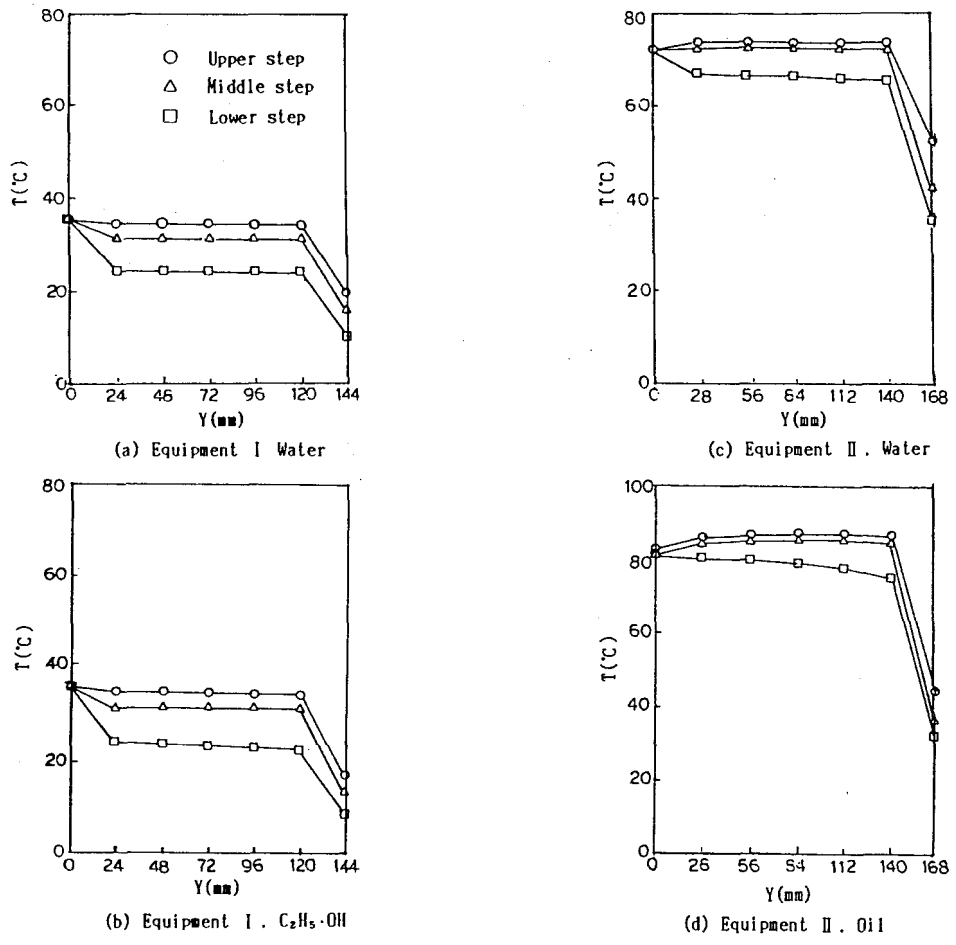

Fig.6 Temperature distribution (T) at the distance of Y from the heating surface. (after 60 min from the run start)

where A_w = cooling surface of the model thermosiphon.

T_{sh}, $T_{s\ell}$ = temperature of the filling layer each contact with the heating and cooling surface of the test bath.

Heat transfer coefficient h obtained by equation (5) means therefore overall heat transfer coefficient of the filling layer including thermal conductivity and heat transfer coefficient by convection of the working fluid. Variation of heat transfer coefficient h and elapsed time of the working fluid in the Equipment I and II are indicated in Fig.7. Heat transfer coefficient h takes large value just after the cooling water is induced to the model thermosiphon, then decreases rapidly in the following 7 to 8 minutes and converges to the steady value in all working fluid.

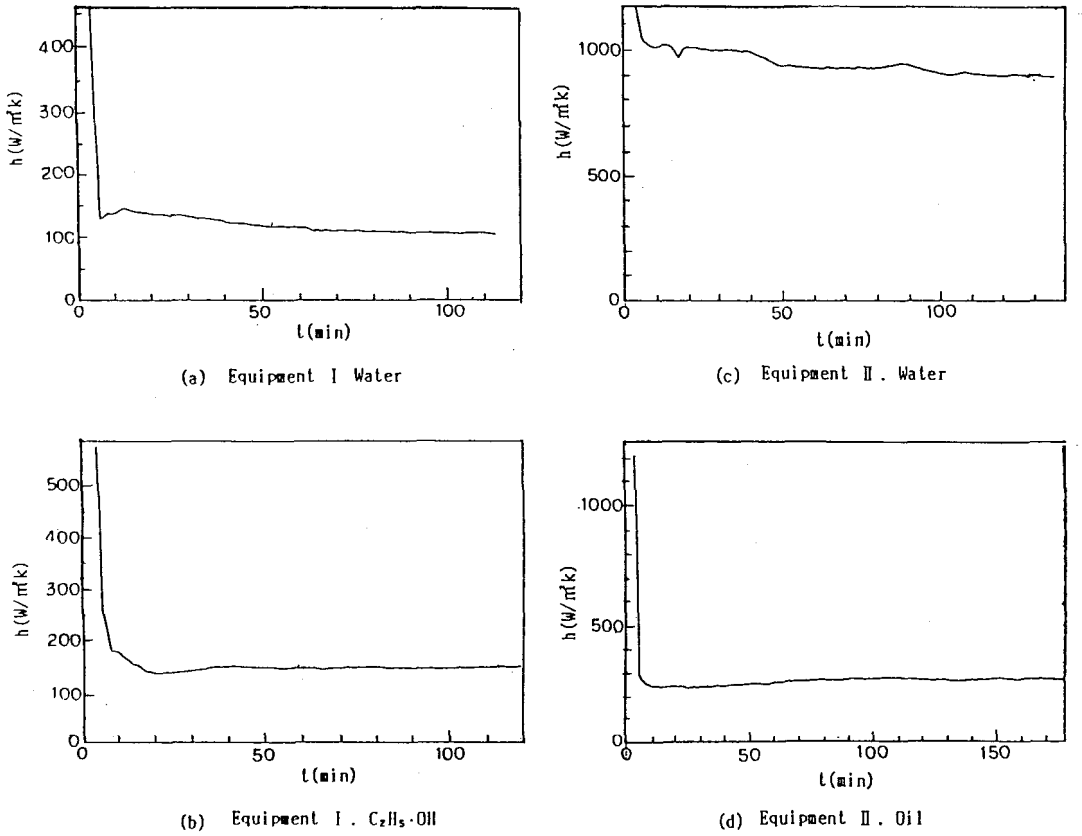

Fig.7 Heat transfer coefficient along the time proceeding

After falling down, heat transfer coefficient rises up again temporarily and reaches finally the steady state of equilibrium Gradient of up growing curve mentioned above in case of water, and alcohol is steep, and slow in oil. The reason of the changing process of the heat transfer coefficient along the time proceeding is considered as follows. The large quantity of heat transfers to the cooling surface from the near layer of the cooling surface by heat conduction just after the cooling water is induced to the model thermosiphon and high heat transfer coefficient can be obtained correspondingly in the first step. Then the heat transfer quantity reduces along the temperature decrease of the filling layer near the thermosiphon and heat transfer coefficient h comes down in the second step. After that, intensive convection of the working fluid takes place based on the temperature difference between the heating surface and cooling surface, then the heat transfer coefficient increases slightly and temporarily in the third step. The value of heat transfer coefficient h then converges into steady value slowly in the final stage.

4.5 Processing for Correlation between Dimensionless Number

Temperature distribution and coefficient of the heat transfer are obtained as described before. It is considered useful that convert the primary data to the correlation of dimensionless number for the purpose of regeneration of the data in case the equipment operates under the different conditions.

(1) Relation between corrected dimensionless Number of Nu^* and Fo^*

Corrected Nusselt Number Nu^* and Fourier Number Fo^* are to be calculated by following process[5-7].

$$Nu^* = h \cdot \ell / \lambda^* \tag{6}$$

$$\lambda^*/\lambda_f = E + (1 - E)/\{\phi + (2/3)(\lambda_f/\lambda_s)\} \tag{7}$$

here

λ^* = effective thermal conductivity in the porous filling layer (W/mK)

ℓ = distance between the heating and cooling surface (m)

where the figure of λ_f , λ_s is obtained by Tables 1 and 2, ϕ is based on ϕ_1, ϕ_2 and E can be calculated by equation (3)

$$\phi = \phi_2 + (\phi_1 - \phi_2)\ (E - 0.26)/0.216 \tag{8}$$

$$\phi_n = \frac{\{(\kappa-1)/\kappa \cdot \sin\Psi_0\}^2/2}{\ell n\{\kappa - (\kappa - 1)\cos\Psi_0\} - (\kappa-1)/\kappa \cdot (1 - \cos\Psi_0)} - \frac{2}{3\kappa} \tag{9}$$

$$\kappa = \lambda_s/\lambda_f$$

$$\sin^2\Psi = 1/N \tag{10}$$

here

ϕ_1 is the value of ϕ when N=1.5 in equation (10)

ϕ_2 is the value of ϕ when $N=4\sqrt{3}$ in equation (10)

(2) Fo^* in the filling layer

$$Fo^* = a^* \cdot t/\ell^2 \tag{11}$$

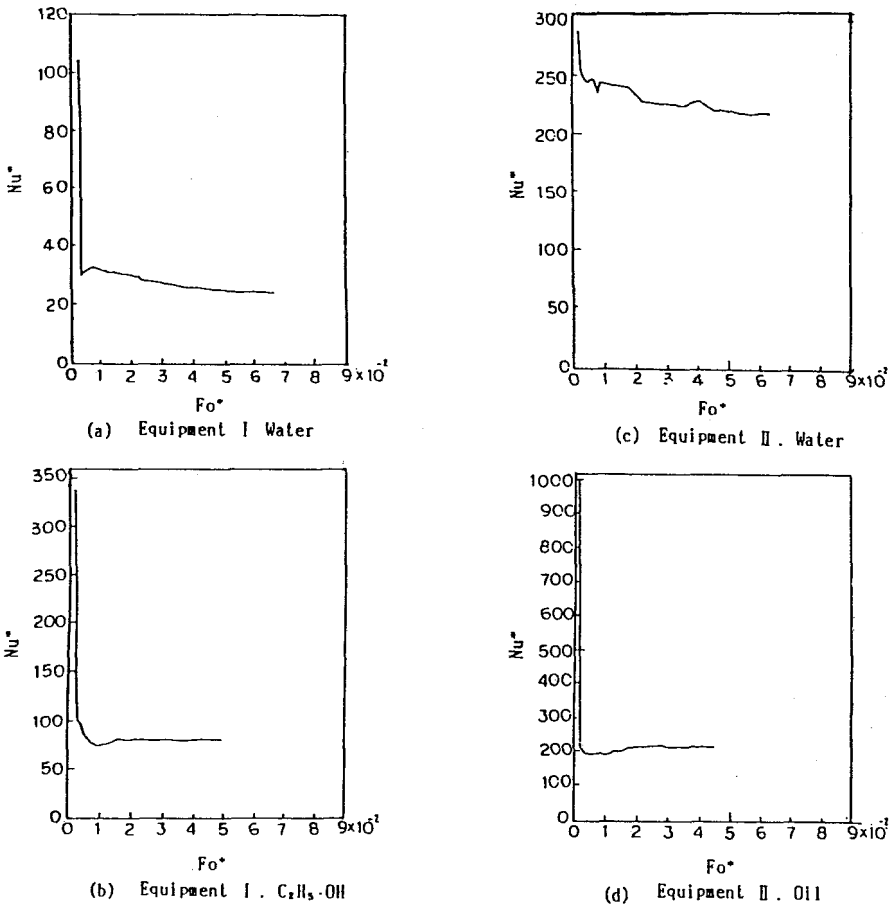

Fig.8 Relation between Nu^* and Fo^*

$$a^* = \lambda^*/(C\rho)^* \tag{12}$$

here

$$(C\rho)^* = (1 - E)(C\rho)_s + E(C\rho)_f \tag{13}$$

Correlation between Fo^* and Nu^* is shown in Fig.8 utilizing the value of Fo^* and Nu^* by equations (6) and (11). Changing process of Nu^* to Fo^* in Fig.8 seems to be resembled closely with the correlation between the change of coefficient h and elapsed time t in Fig.7.

(3) Relation between Fo^* and Ra^*

Corrected Rayleigh Number in filling layer Ra^* is calculated by

$$Ra^* = Ra \cdot S_i / \ell^2 \tag{14}$$

where $Ra = Gr \cdot Pr = \ell^3 \cdot g \cdot \beta \Delta T / \nu^2 (\nu / a^*)$

Relation between Fo^* and Ra^* by equation (11) and (14) is shown in Fig.9.

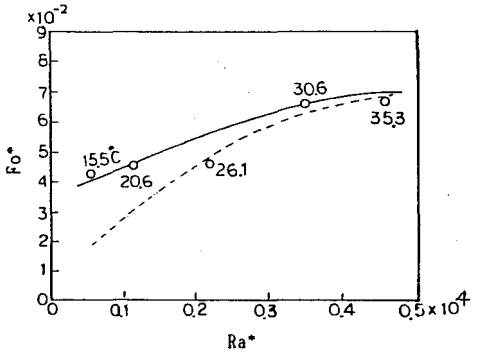

(a) Equipment I Water

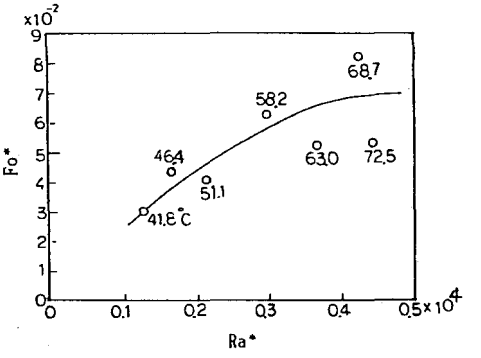

(d) Equipment II. Water

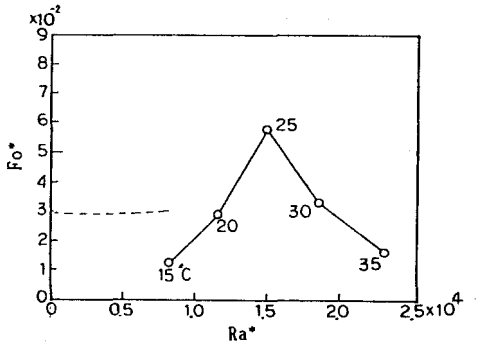

(b) Equipment I. $C_2H_5 \cdot OH$

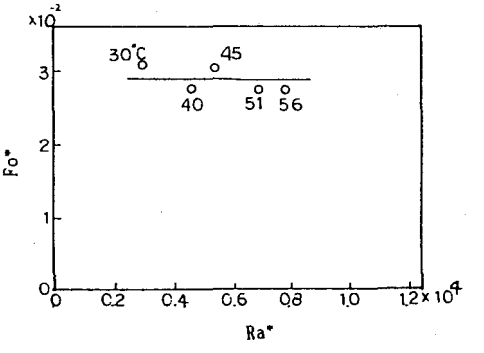

(e) Equipment II. $C_2H_5 \cdot OH$

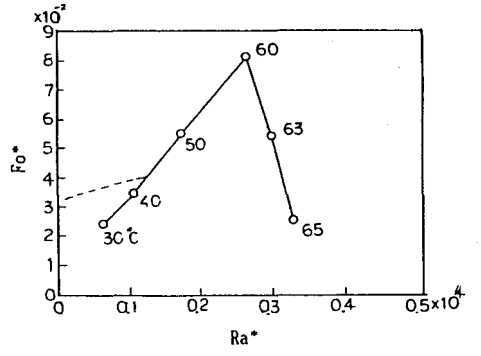

(c) Equipment I. Oil

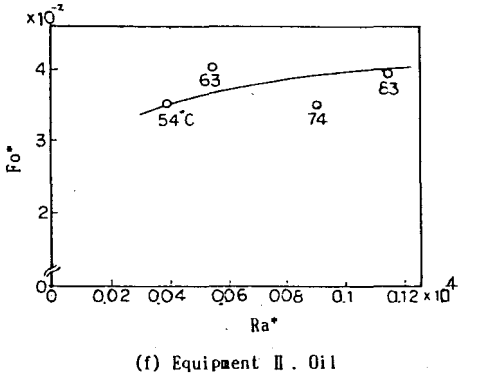

(f) Equipment II. Oil

Fig.9 Relation between Fo^* and Ra^*

In Fig.9, (a) (d) shows the relation of Fo^* and Ra^* in the Equipment I and II respectively the case of water, (b) (e) and (c) (f) indicate the case of alcohol and oil. The dotted line of (a) (b) (c) in Fig.9 (shows the case of Equipment I) indicates the value of Fo^* in (d) (e) (f) (shows the case of Equipment II) so as to understand the relative situation of Fo* values in both Equipment I and Equipment II. The figure of Fo^* on the vertical axis shows the elapsed time required to reach equilibrium, and the figure of Ra^* on the horizontal axis means the intensity of natural convection of the working fluid. Figure of the temperature written on the line of the Fo^* Number in Fig.9 means the starting temperature of the heating surface. According to Fig.9 Fo^* Number increases and converges to a certain value in case of water, but it changes from increase to decrease at a certain value of Ra^* Number ($Ra^* = 0.25\times 10^4$) in case of oil in Equipment I. Similar phenomenon is observed in case of alcohol at the Ra^* Number of 1.5×10^4.

The reason of this is considered that longer elapsed time is required to reach the thermal equilibrium to transport larger accumulated heat quantity in the filling bath when the temperature difference between the heating and cooling surface becomes large. The convection of the working fluid is activated at the same time, however, and two opposite components are canceled to each other and then Fo^* Number converges to a certain value or changes from increase to decrease as in Fig.9. Fo^* Number of water does not change from increase to decrease in the range of this experiment ($Ra^* \leqq 0.5 \times 10^4$) as indicated in Fig.9 (a) (d), but it can be estimated that the figure of Fo^* Number begins to decrease in the range of $Ra^* \geqq 0.5 \times 10^4$ and Fo^* has maximum value of 0.07 at around the value of $Ra^* = 0.5 \times 10^4$ correspondingly.

5. CONCLUSION

The extract system of geothermal heat with two phase closed thermosyphon and measurement of heat transfer coefficient are studied experimentally utilizing porous filling layer and model thermosiphon. Following subjects are induced as the conclusion.

(1) Sudden dropping of temperature occurs in the near layer of cooling surface just after the cooling water is induced to the model thermosiphon and temperature of the rest parts of the filling layer decrease slowly to the stable state finally.
(2) The temperature gradient in the layer near the cooling surface is largest on radial direction compared with the other part of the layer.
(3) The tendency described in (1) and (2) above is common phenomenon through the experiment regardless of the working fluid and the type of the equipment.

(4) Heat transfer coefficient drops suddenly just after cooling water is induced to the thermosiphon, and decreases slowly to the final equilibrium.

(5) On the way of decreasing of heat transfer coefficient h, temporary rising process exists in short time and then converges into stable value finally. Temporary rising process appears suddenly and in short time in case of water and alcohol; indefinitely in case of oil.

(6) Similar tendency of the phenomenon as in (5) is observed in the relation between corrected Nusselt Number Nu^* and Foulier Number Fo^*.

(7) Fo^* number increases slowly and converges to a certain value with the increase of Ra^* number in case of water. However, it was found that Fo^* changes from increase to decrease at a certain Ra^* Number in case of alcohol and oil.

REFERENCES

(1) Tien, K. C., Zarling, J. P. "Review on Application of Heat Pipe and Thermosiphon in Cold Area" Proceedings of Japan Association of Heat Pipes, pp. 46-74 (1991)

(2) Mizuno, S. Akagawa, K. Kutsuna, T. Matsui, N. Ito, K. Kato, T. Hangai, M. "Long-Term Storage of Solar Energy Underground and Use for Vinylhouse Heating," Refrigeration, 57-654, pp.349-357 (1982)

(3) Matsui, N. Mizuno, S. Akagawa, K. Kutsuna, T. Ito, K. Kato, T. Hangai, M. "Green House Heating with Thermosiphon Heat Pipes for long Term Underground Storage System of Solar Energy" Reprint of Memories of the Faculty of Engineering, Post graduate course of Natural Science of Kobe Univ, 1-B, 1-16, ppl-14 (1983)

(4) Japan Association of Heat Pipes (Negishi, Oshima, Itoh), "Practical Heat Pipes", published by Nikkan Kogyo Shinbunsha, pp.184-190,(1985)

(5) Kunii, D. "Unit Operation by Thermal Technique" 1st Edit. published by Maruzen Co., Ltd. pp.136-139 (1976)

(6) JSME Data Book, Heat Transfer, 3rd Edition pp.227-228 (1975)

(7) Warren H, Gidt "Principles of Engineering Heat Transfer" published by Maruzen Co., Ltd. p.264 (1960)